Iran. J. Biotechnol. October 2022;20(4): e3154 DOI: 10.30498/ijb.2022.305258.3154

Research Article

Use of Gelatin as a Sacrificial Agent in Combination with Ultrasonication to Improve Cell Infiltration and Osteogenesis of Nanofibrous PCL-nHA Scaffolds for Bone Tissue Engineering

Saeed Moghadam Deymeh[1], Sameereh Hashemi-Najafabadi[1,*], Mohamadreza Baghaban-Eslaminejad[2,], Fatemeh Bagheri[3]**

[1]Biomedical Engineering Department, Faculty of Chemical Engineering, Tarbiat Modares University, Tehran, Iran
[2]Department of Stem Cells and Developmental Biology, Cell Science Research Center, Royan Institute for Stem Cell Biology and Technology, ACECR, Tehran, Iran
[3]Biotechnology Department, Faculty of Chemical Engineering, Tarbiat Modares University, Tehran, Iran

[*]*Corresponding author*: Sameereh Hashemi-Najafabadi, Biomedical Engineering Department, Faculty of Chemical Engineering, Tarbiat Modares University, Tehran, Iran. Tel.: +98-2182884384, Fax: +98- 2182884931, E-mail: s.hashemi@modares.ac.ir

[**]*Co-Corresponding author*: Mohamadreza Baghaban-Eslaminejad, Department of Stem Cells and Developmental Biology, Cell Science Research Center, Royan Institute for Stem Cell Biology and Technology, ACECR, Tehran, Iran. Tel: +98-2123562524, Fax: +98-2123562507, E-mail: eslami@royaninstitute.org

Background: Electrospinning has been widely used to prepare nanofibrous scaffolds for bone tissue engineering. However, owing to the small pore size of electrospun scaffolds, cellular infiltration and tissue ingrowth are impossible. The use of sacrificial fibers (like poly ethylene oxide (PEO)) in combination with ultrasonication has been an appropriate way to increase the pore size of the electrospun scaffolds in our previous work. However, it is uneconomical due to the high cost of PEO.

Objectives: In this study, gelatin was chosen as a novel sacrificial agent in co-electrospun with polycaprolacton-nanohydroxyapatite (PCL-nHA).

Materials and Methods: After electrospinnig, gelatin was washed with water, and the prepared scaffold was ultrasonicated. Morphological and structural properties of the prepared scaffolds were studied by SEM. Fourier transform infrared (FTIR) spectroscopy and water contact angle analysis were used to evaluate the removal of gelatin.

Results: According to the SEM results, the pore size of the modified scaffolds was increased 3-folds compared to the control sample. For PCL-nHA: gelatin (80:20) after the treatment, the average cell infiltration was 42.7 µm, while there was no infiltration for the control group. The modified electrospun scaffold significantly enhanced the osteogenic differentiation of hBMSCs as verified by increased ALP activity and upregulation of runt-related transcription factor 2 (RUNX2), collagen type 1 (COL1) and osteocalcin (OCN) genes.

Conclusion: Co-electrospun PCL-nHA with gelatin as a sacrificial agent in combination with ultrasonication may be an effective, economic and controllable method to increase the pore size in electrospun scaffolds for bone tissue engineering applications.

Keywords: Electrospinning, Gelatin, Osteogenic Differentiation, Polycaprolacton-Nanohydroxyapatite (PCL-nHA)

1. Background

Bones, as the most important structural part of the body, are prone to fracture and injurie. Bone tissue repairing by itself is limited to small bone defects. Clinical practices in bone grafting have been widely used in the case of large bone defects. Unfortunately,

allografts and autografts have many drawbacks, such as infection in the host, immune responses, long-term surgery and limited donors (1-6). Owing to limitations in traditional methods, tissue engineering has been introduced as a promising therapeutic approach to regenerate the damaged bones (7-10). Bone scaffolds have played a crucial role in making the structure for maturing of tissue engineered constructs. In addition to biocompatibility and osteogenesis, a bone scaffold should have interconnected microarchitecture to promote cell infiltration and development of bone extracellular matrix (ECM) (11).

Electrospinning has gained considerable attention due to production of nonwoven textile mimicking the topography of natural extracellular matrix (ECM) and simplicity of performance. However, owing to the small pore size of electrospun scaffolds, cellular infiltration and tissue ingrowth into scaffolds are impossible (12-15). With conventional electrospinning techniques, the fabricated scaffold provides 2D nanostructure morphology. In addition, multilayered electrospun constructs are more reasonable for bone tissue engineering in deep defects and need a larger pore size. In this case, pore size and their interconnection are vital for both cell infiltration and diffusion of oxygen and nutrients (16, 17).

Mesenchymal stem cells (MSCs) are multipotent progenitor cells that capable of differentiation into bone, cartilage and fat under specific culture conditions. Osteogenesis is characterized by deposition of calcified matrix, increasing in alkaline phosphatase activity (ALP), expression of related bone specific markers like osteocalcin (OCN), osteopontin (OP) and Runx2. For suitable therapeutic manipulation of MSCs in bone tissue engineering, it is necessary to utilize osteoinductive scaffolds. The use of nano hydroxyapatite (nHA) as a osteoinductive material has been extensively reviewed in the literature. Polycaprolactone (PCL) has been widely used in the fabrication of 2D and 3D scaffolds in bone tissue engineering due to its advantage like good mechanical properties, biocompatibility and suitability for modification (18, 19).

Pore size can be increased by increasing the fibers diameters in electrospun scaffolds. It has been shown that larger fiber diameters reduced cell adhesion compared to small diameter fibers (20). Using several methods, such as modified collector design, ultrasonication (postelectrospinning), surface conductivity ablation and use of sacrificial fibers, it has been attempted to increase the pore size of electrospun scaffolds and to enhance cell infiltration. Electrospun scaffolds with enhanced pore size have been shown to improve cell expansion and proliferation compared with conventional electrospun scaffolds (21). Poly ethylene oxide (PEO) is the most popular sacrificial agent easily dissolved in an aqueous solution for removal. By increasing the amount of PEO removed from the scaffolds, the cell infiltration has increased. Although the number of cells migrated into the scaffolds increases by PEO removal, the mechanical strength decreases (22-28). Sacrificial fibers, including PEO in combination with ultrasonication, were an appropriate way to increase the pore size of the electrospun scaffolds in our previous work (14). However, due to the high cost of PEO, it is an unsuitable option in many applications.

Gelatin is a natural biopolymer used in electrospun scaffolds, and similar to PEO, it is water soluble. Owing to its poor mechanical properties, it is used mostly in compositions with a synthetic polymer, such as PCL, poly lactic-co-glycolic acid (PLGA) and polyethylene glycol (PEG). Gelatin has several applications in tissue engineering and convenient electrospinning, also shows rapid dissolution in water and is commercially available at a relatively lower cost. Then, the idea that it is investigated as a sacrificial component has been developed (29-31).

2. Objectives

This study investigated the potential of gelatin as a novel sacrificial agent to increase the pore size of electrospun polycaprolactone-nanohydroxyapatite (PCL-nHA) scaffolds. To date, no article has investigated these study to increase the pore size of electrospinning scaffolds in bone tissue engineering. After gelatin removal, ultrasonication was used to further increase the pore size. PCL-nHA scaffolds were characterized by different chemical and mechanical methods, and then human bone marrow mesenchymal stem cells (hBMSCs) were seeded on them and exposed to osteogenic conditions.

3. Materials and Methods

3.1. Materials

Gelatin type A (Approx. 300 Bloom) from the porcine skin in powder form, PCL (Mn=80 kD), and nHA

(nanoparticle size <200 nm) were purchased from Sigma-Aldrich Company. Chloroform, acetic acid and N, N-dimethyl formamide (DMF) were purchased from Merck Company. Phosphate buffered saline (PBS), Dulbecco Modified Eagle's Medium (DMEM), fetal bovine serum (FBS) and trypsin/EDTA were obtained from GIBCO. MTT (3-(4,5-dimethylthiazol-2-yl)-2,5-diphenyltetrazolium bromide), DAPI (4,6-diamidino-2-phenylindole) and antibiotics (penicillin-streptomycin) were supplied from Sigma-Aldrich Company.

3.2. Preparation of Electrospun Scaffolds

3.2.1. Preparation of PCL-nHA and Gelatin Solutions

PCL-nHA solution was prepared by adding 7.5% (w/w) of nHA to 12% (w/v) PCL solution in chloroform/DMF (4:1 v/v) by stirring at 500 x g for 4 hours. The blended solution was sonicated for 15 minutes until nHA was completely dispersed in the PCL solution. Gelatin was dissolved in 40% (v/v) acetic acid by stirring for 2 hours to obtain a 25% (w/v) solution. All the polymer solutions were prepared at room temperature.

3.2.2. Co-electrospinning

Gelatin solution and PCL-nHA suspension were co-electrospun on a rotating collector from two separated spinners. Each polymer solution was loaded into a separated 10 mL syringe and then delivered at a constant flow rate ($Q=0.5\ mL.h^{-1}$) by a syringe pump. Electrospinnig was performed under these conditions: high voltage, 17 kV; drum speed, 30 x g; and distance between the needle and the drum, 16 cm. After electrospinning, the prepared sheets were punched as 15 mm in diameter. Water (ambient temperature) was used as a solvent to remove the gelatin fibers. To find the optimized ratio of PCL-nHA and gelatin, the samples were weighed before and after washing, and the amount of lost weight was calculated. The gelatin removal process was performed in 3 consecutive days by changing water daily. Then, using ultrasonication, the scaffold pore size was increased according to our previous work (14). In this study, two groups with the ratios of 90:10, and 80:20 of PCL-nHA: gelatin in combination with ultrasonication were investigated.

3.3. Scaffolds Morphology

The morphology of PCL-nHA electrospun scaffolds was studied using SEM. The samples were coated with gold and observed with a scanning electron microscope (Tescan Mira 2 LMU, Czech Republic). Twenty-five different fibers from different places of each image were randomly selected, and then the average fiber diameter and pore area were calculated using the image J analysis software. The fiber diameter, pore size and pore area were reported as the mean ± standard deviation (SD).

3.4. Mechanical Properties

Tensile test was conducted for the electrospun scaffolds using a mechanical test machine (Santam, STM20, Iran) with the load cell of 10 N and cross-head speed of 10 $mm.min^{-1}$. The scaffolds were cut in dimensions of 10×50 mm. The tensile modulus was measured by the stress-strain curve slope in its initial linear section (n=3).

3.5. Contact Angle Measurement

Wettability of the scaffolds was investigated using the drop shape method (contact angle measurement) at room temperature. For this purpose, 5 µL of water was placed on the surface of each scaffold, and the value of contact angle was calculated by an optical contact angle measuring system (Rame- Hart Instrument, USA). Some of the scaffolds were also modified by the oxygen plasma treatment to investigate the hydrophilicity. The contact angle measurement was performed in 5 different places of the scaffold for each sample.

3.6. FTIR

FTIR spectroscopy was performed using PerkinElmer Spectrum (USA) to analyze the removal of gelatin as sacrificial fibers from scaffolds. FTIR spectra were prepared using a Perkinelmer Frontier FTIR spectrometer.

3.7. Cell Culture and Seeding on the Scaffolds

hBMSCs (passage 3) were prepared from Royan Institute (Tehran, Iran) and maintained in high glucose DMEM, supplemented with 10% (v/v) FBS and 1% penicillin/streptomycin. Sterilization was performed by soaking the scaffolds twice in 70% ethanol for 30 min, followed by UV irradiation and rinsed with sterile PBS and then dried. The samples were incubated in a humidified atmosphere containing 5% CO_2 and 37 °C. The cells were seeded on the scaffolds (20,000 cells/scaffold) inside 24-well plates and incubated at 37 °C and 5% CO_2. To examine the differentiation of hBMSCs,

the cell seeded scaffolds were incubated at 37 °C and 5% CO_2 in an osteogenic medium up to 14 days. The osteogenic medium containing 0.1 µM dexamethasone, 10 mM b-glycerophosphate and 50 µM ascorbic acid in DMEM was used.

3.8. MTT Assay

The viability of hBMSCs on the scaffolds was assessed using the MTT assay in 24-well tissue culture plates. After 7, 14 and 21 days, the medium was removed from each well, and the samples were incubated in the medium containing the MTT solution (5 $mg.mL^{-1}$). After 3 hours, formazan crystals were dissolved in 200 µL DMSO, and the absorbance was read using an ELISA microplate reader (Thermo Scientific, USA) at 570 nm (n=3).

3.9. Cell Infiltration into the Scaffolds

The scaffolds were seeded at a density of 2×10^4 cells/scaffold in 24-well plates and incubated for one week. Then, to investigate infiltration, the cell cultured scaffolds were fixed in a 30% (w/w) formalin-sucrose solution for 24 hours. The fixed scaffolds were frozen in an optimal cutting temperature compound (OCT, Finetek, Torrance, CA), followed by cutting into 10 µm sections using a Leica cryostat-micro-tome. Then, the sections were stained with DAPI to visualize the location of cell nuclei using a fluorescence microscope (BX51, Japan).

3.10. Alkaline Phosphatase (ALP) Activity

ALP activity as an early marker of osteoblastic phenotype and bone differentiation was measured using the ALP assay kit according to the manufacturer's instructions (Bio Vision, USA). Total protein content using the BCA protein assay kit (Thermo Scientific, USA) was measured. ALP activity was calculated by a standard curve and normalized against the total protein.

3.11. Morphological Study of the Cell-seeded Scaffolds

SEM imaging was used to investigate the morphology of hBMSCs cultured on the scaffolds. The scaffolds were placed in 24-well plates, and 20,000 cells were poured on each scaffold and incubated at 37 °C and 5% CO_2. After 7 days, the cell-scaffold constructs were fixed by 2.5% glutaraldehyde for 48 hours, and then washed with PBS and lost their water in alcohol graded series. Finally, they were dried overnight, and then coated with a thin layer of gold and analyzed at high voltage by SEM (Tescan Mira 2 LMU, Czech Republic).

3.12. Gene Expression Analysis

The cell differentiation was evaluated using reverse transcription-polymerase chain reaction (RT-PCR) to evaluate the expression of bone-related genes, such as osteocalcin (OCN), runt-related transcription factor 2 (Runx 2), and collagen type I (COL I), after 14 days in the osteogenic medium. Briefly, total RNA extraction was carried out by Trizol/chloroform (Qiagen, USA) according to the manufacturer's protocol. cDNA was synthesized using isolated RNA and amplified by specific primers. To evaluate the expression of osteogenic markers, the SYBR Green PCR Master Mix assay was used to perform real-time quantitative RT-PCR. The expression value of the osteogenic markers was normalized by GAPDH as the reference gene. The RT-PCR primers used are listed in **Table 1**.

3.13. Statistical Analysis

The quantitative data were performed as mean ± SD and analyzed using student's t-test, and the significant level was set at the p-value < 0.05. All experiments were conducted at least 3 times.

Table 1. Real Time RT-PCR Primer Sequence

Gene	Primer sequence	
COL I	F: 5′CTGCAAGAACAGCATTGCAT3′	R: 5′-GGCGTGATGGCTTATTTGTT-3′
OCN	F: 5′GTGCAGAGTCCAGCAAAGGT3′	R: 5′TCAGCCAACTCGTCACAGTC3′
Runx2	F: 5′AACCCACGAATGCACTATCCA3′	R: 5′CGGACATACCGAGGGACATG3′
GADPH	F: 5′CCAGGTGGTCTCCTCTGACTTC3′	R: 5′GTGGTCGTTGAGGGCAATG3′

4. Results

4.1. Morphological Analysis

Gelatin and PCL-nHA nanofibers were separately prepared by the electrospinning method. Various parameters, such as the flow rate, the polymer solution ratio, the applied voltage, and the needle to the collector distance, were fixed as previously mentioned. The average diameter of PCL-nHA and gelatin fibers was 1230 ± 270 and 148 ± 55 nm, respectively.

4.2. Co-electrospinning of PCL-nHA and Gelatin

In the co-electrospinning of PCL-nHA and gelatin, two syringes were at a constant distance from each other, and then, different sections of the sheet had different ratios of two polymers. Due to using a syringe pump with moving syringes, to obtain a different percentage of PCL-nHA and gelatin, different sections of the electrospun sheet were cut and weighted to determine the actual ratio of polymers. The morphology of the scaffolds before and after the treatment (gelatin removal from the scaffolds by dissolving in water and ultrasonication) are shown in **Figure 1**.

Total pore area was increased 2.5-2.8-fold compared to the unmodified scaffolds (**Table 2**). Although an increase in the pore areas for two specimens was

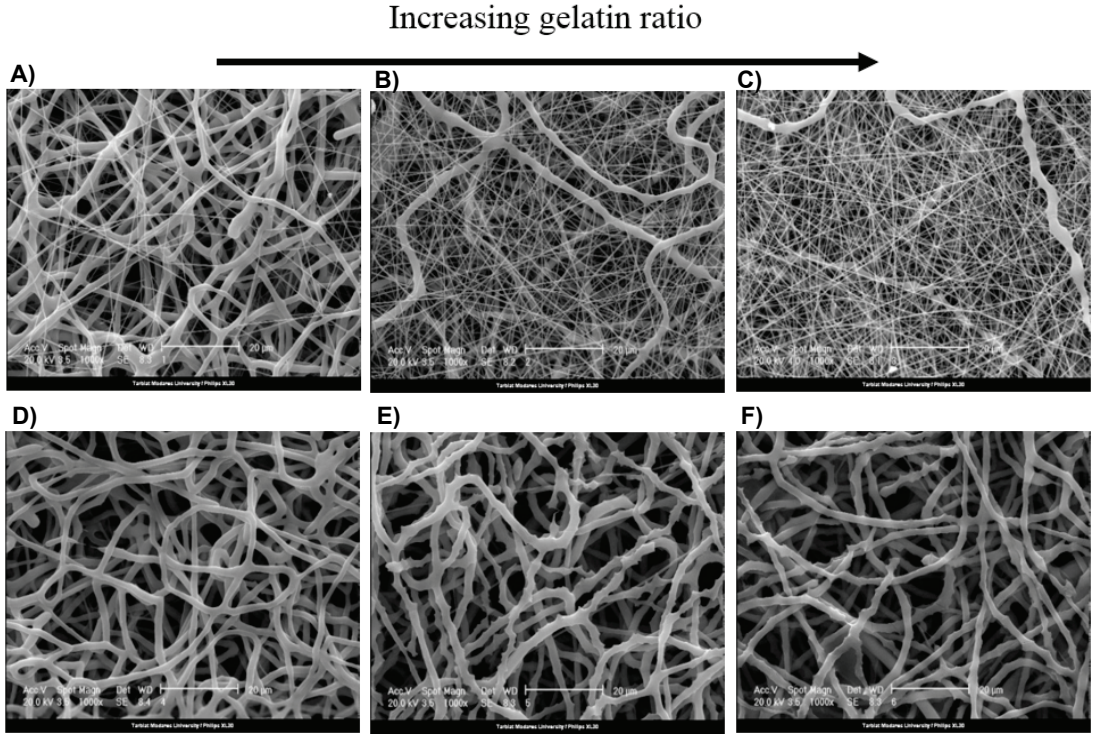

Figure 1. SEM images of co-electrospun scaffolds (**A, B, C**) before and (**D, E, F**) after the treatmet (gelatin removal and ultrasonication). By increasing the gelatin ratio in the scaffolds, larger pores were created. (**A, D**) PCL-nHA:gelatin (90:10) before and after the treatment. (**B, E**) PCL-nHA:gelatin (80:20) before and after the treatment, and (**C, F**) PCL-nHA:gelatin (70:30) before and after the treatment

Table 2. Total pore areas before and after the treatment for different weight ratios of PCL-nHA:gelatin

Weight ratio of PCL-nHA: gelatin	Total pore area before the treatment (μm^2)	Total pore area after the treatment (μm^2)
90:10	547±21	931±35
80:20	345±32	1033±54
100:0 (control)	369±25	-

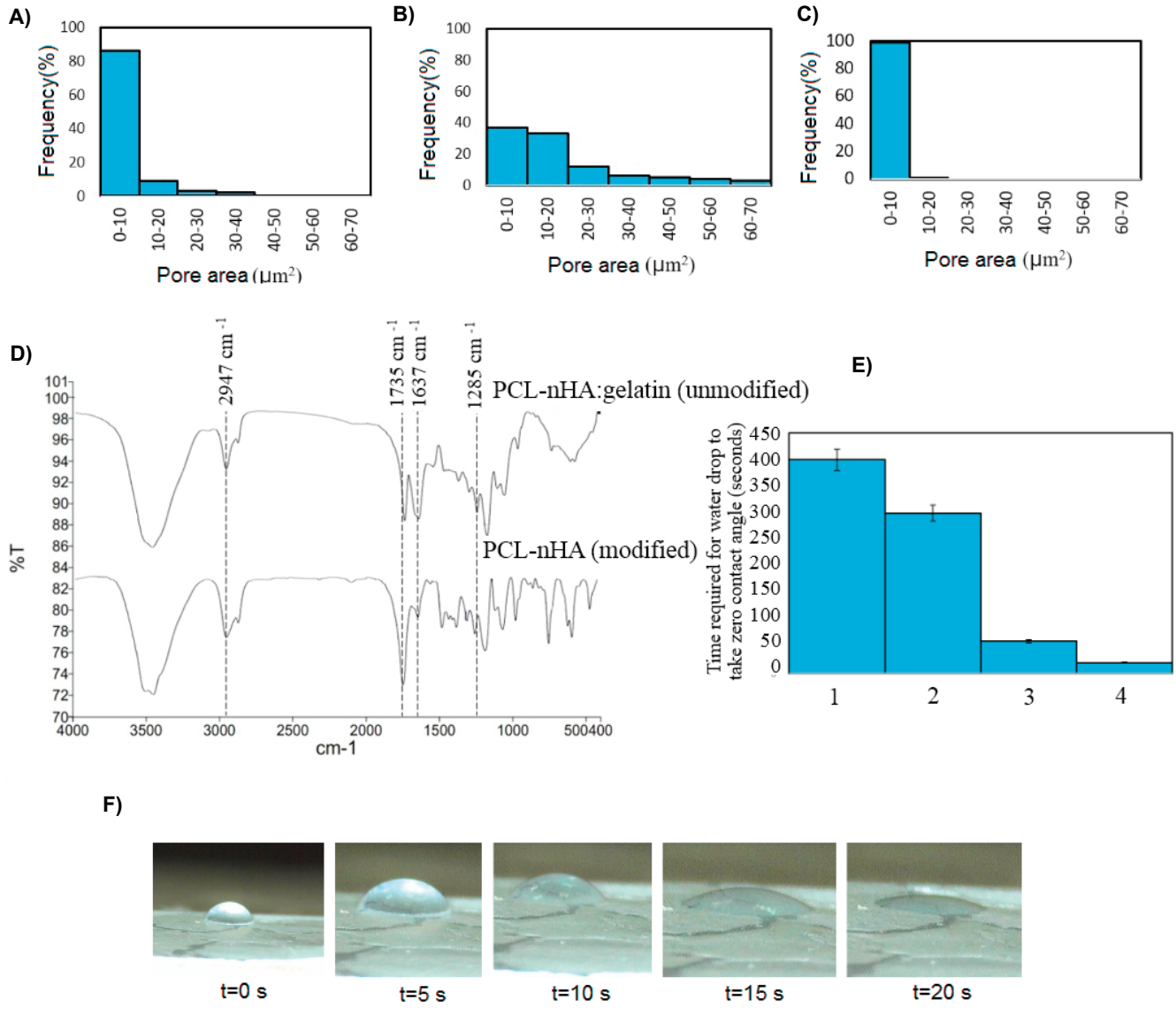

Figure 2. Distribution of the pore size in the modified PCL-nHA:gelatin scaffolds **A)** 90:10, **B)** 80:20, **C)** 100:0 (control), **D)** FTIR curves of PCL-nHA:gelatin (80:20, unmodified) and PCL-nHA (modified), **E)** The time required for the water drop to take a zero contact angle on the surface of different groups (1) after gelatin removal, without plasma treatment, (2) before gelatin removal, without plasma treatment, (3) after gelatin removal, with plasma treatment and (4) before gelatin removal, with plasma treatment, **F)** Drop contact angle changes with respect to time for the sample scaffold, before gelatin removal and with plasma treatment.

similar, the pore area distribution was different from each other. The distribution of pore size in PCL-nHA: gelatin (90:10 and 80:20) after the treatment and in the control group (PCL-nHA unmodified scaffold) are shown in **Figure 2A-2C**. As can be seen, by increasing the percentage of gelatin, as a sacrificial agent, the frequency of the pores with higher areas were increased.

4.3. FTIR Analysis

FTIR spectroscopy analysis was conducted to determine the chemical composition of the scaffolds and evaluate the removal of gelatin (**Fig. 2D**). Here, several PCL-nHA characteristic bands are clearly observed in 2947 (asymmetric stretching-CH2), 1735 (carbonyl stretching), 1285 (C-O and C-C stretching) and 1161 cm^{-1} (C-O-C, symmetric stretching). The FTIR

spectra show a number of characteristic bands for HA nanoparticles. Additionally, 3571 and 631 cm^{-1} bands are related to the tensile mode of hydrogen-bonded OH-ions and the liberation mode of OH-ions, respectively. Furthermore, 1041, 570 and 601 cm^{-1} bands are related to PO_4 groups. The characteristic band of gelatin is related to N-H stretching at 3433 (amide band), C=O stretching in 1637 (amide I), N-H bending in 1543 (amide Ⅱ), and N-H in 559 cm^{-1}. The corresponded peaks in the modified samples, which are related to the presence of gelatin, shifted to the wavelength lower than the one in the unmodified sample (before gelatin removal), indicating the partial removal of gelatin fibers upon immersion in water.

4.4. Analysis of Surface Hydrophilicity

In this experiment, four groups were studied to determine whether plasma treatment is required after gelatin removal. Four groups of PCL-nHA:gelatin (80:20) were investigated of which two groups were without plasma treatment (one group containing gelatin and the other after gelatin removal). The other two groups, initially, had plasma treatment, which then, one was with gelatin removal and one without gelatin removal. The time required for the water drop to disappear and take a zero contact angle on the surface of the scaffolds is shown in **Figure 2E**. The images of the drop at specific intervals for the groups are shown in **Figure 2F**. Owing to incomplete removal of gelatin, all of the scaffolds were hydrophilic, even after gelatin removal. Plasma treatment considerably enhanced the hydrophilicity of the scaffolds, and water drops on the plasma treated scaffolds disappeared immediately.

4.5. Mechanical Properties

Mechanical properties of the electrospun scaffolds were measured by the stress-strain curves. To assess the mechanical properties of the modified scaffolds (after rinsing and ultrasonication), two groups from different weight ratios of modified PCL-nHA: gelatin (90:10 and 80:20) and a control sample (PCL-nHA) were selected. These two ratios were investigated with respect to our previous work in which the optimized polymer weight ratio of PCL-nHA: PEO was 80:20 to achieve suitable mechanical properties and appropriate pore size for cell infiltration (14). The mechanical properties of the scaffolds were affected by the treatment modification (gelatin removal and ultrasonication) (**Table 3**) . The young's modulus of 90:10 and 80:20 ratios of the modified PCL-nHA: gelatin was 1.95 and 1.61 MPa, respectively. The relative stress presented in **Table 3** is obtained by dividing the peak stress in each group by the peak stress of the control sample.

4.6. MTT Assay

The viability of hBMSCs was measured in PCL-nHA: gelatin (90:10, 80:20) scaffolds after the treatment in the control groups (tissue culture plate (TCP) and unmodified scaffolds). The results indicated that cell proliferation on the modified nanofibrous scaffolds was higher than that on the TCP and unmodified scaffold. The viability has increased for each group compared to TCP on day 7 (**Fig. 3A**). On day 14, a higher proliferation rate was observed in PCL-nHA: gelatin (80:20) after the treatment compared to PCL-nHA without treatment and cell culture plate ($P<0.05$). After 21 days of culture, a significant difference was found between the modified scaffolds and the control groups. These results demonstrated that the prepared scaffolds were not toxic for the cells and may enhance the cell proliferation.

Table 3. Tensile test results for two groups of the modified scaffolds (PCL-nHA:gelatin 90:10 and 80:20) and control group

Weight Ratio of PCL-nHA:gelatin	Young's Modulus (MPa)	Peak Stress (MPa)	Relative Stress
90:10	4.11 ± 0.21	1.95 ± 0.05	0.77
80:20	3.58 ± 0.15	1.61 ± 0.16	0.64
100:0 (Control)	5.27 ± 0.18	2.51 ± 0.09	1

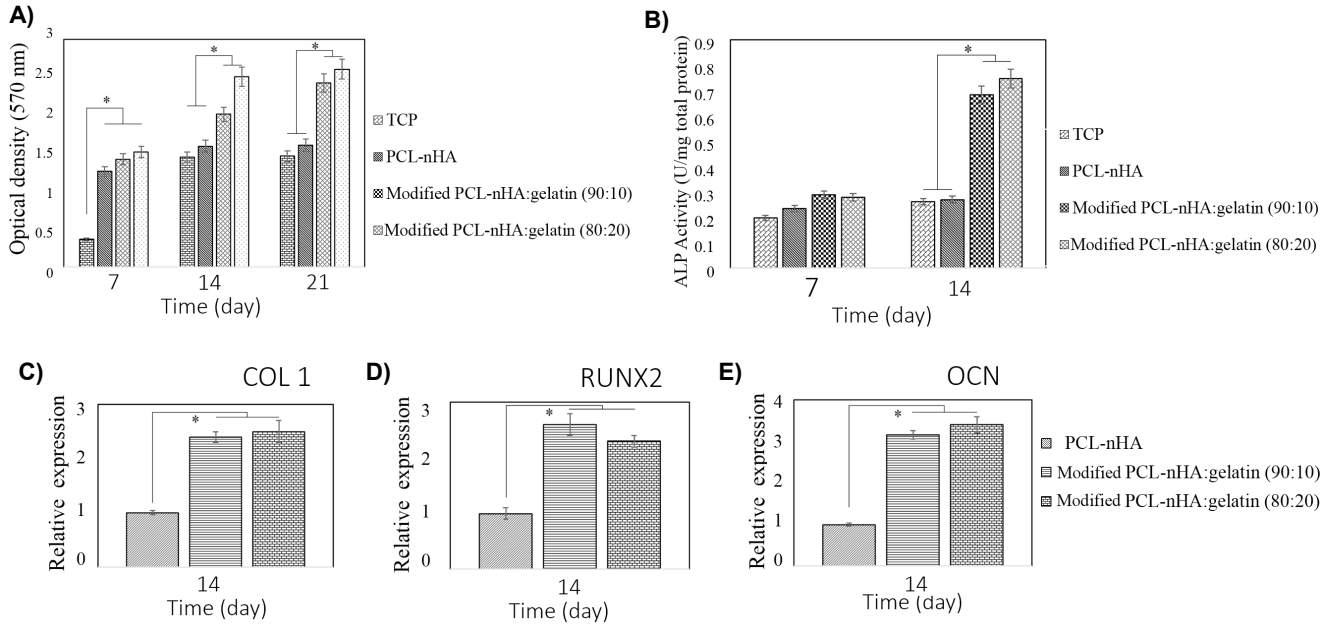

Figure 3. A) Cell proliferation and viability using the MTT assay after 7, 14 and 21 days of culture, **B)** Alkaline phosphatase activity of hBMSCs in different groups, The results of expression of **C)** COL1, **D)** runx2 and **E)** OCN for hBMSCs in different groups after 14 days of culture. (*p<0.05)

4.7. ALP Analysis

ALP as an active enzyme is an important marker in hard tissue formation. The ALP activity of the cells cultured on TCP, unmodified and modified PCL-nHA scaffolds on days 7 and 14 measured (**Fig. 3B)**. There was no significant difference between ALP activity in the culture plate and the scaffolds on day 7 (P>0.05). The was not significantly different between). On day 14, the ALP activity was higher on the modified scaffolds than on the unmodified PCL-nHA and TCP (P<0.05). The ALP activity did not significantly differ between the two modified scaffolds on day 14 (P>0.05).

4.8. Cellular Infiltration

Cell infiltration into the control and modified scaffolds was evaluated by DAPI staining. Cell infiltration values were obtained by averaging the location of cell nuclei in 45 images using the Image J software. As expected, by increasing the amount of sacrificed gelatin from the scaffolds and thus increasing the pore size and interconnection, the cell infiltration was increased. No infiltration was observed for the control group (**Fig. 4A-4C)**.

4.9. Cell Morphology on the Scaffolds

After 7 days of cell culture, SEM images were taken to study cell adhesion and morphology on nanofibrous scaffolds. The cells were well attached and distributed on the scaffolds (**Fig. 4D-4F)**. Higher cell proliferation and spreading were observed on the surface of the modified scaffolds. By increasing the amount of sacrificial gelatin and the related pore size, higher cell attachment and density were observed on the surface of 80:20 than on 90:10 modified scaffolds, being in agreement with the MTT assay results.

4.10. Real Time RT-PCR

To investigate the osteogenic differentiation, real time RT-PCR was performed to assess the expression of bone-related genes, such as osteocalcin (OCN), Runt-related transcription factor 2 (RUNX2) and collagen type 1 (COL1), after two weeks of culture. It is well known that runx2 is a key transcription factor for mineralization and osteoblast differentiation. Collagen type 1 is the major organic part of the bone ECM, and osteocalcin is a late-stage marker for osteogenic differentiation. The RT-PCR analysis indicated that

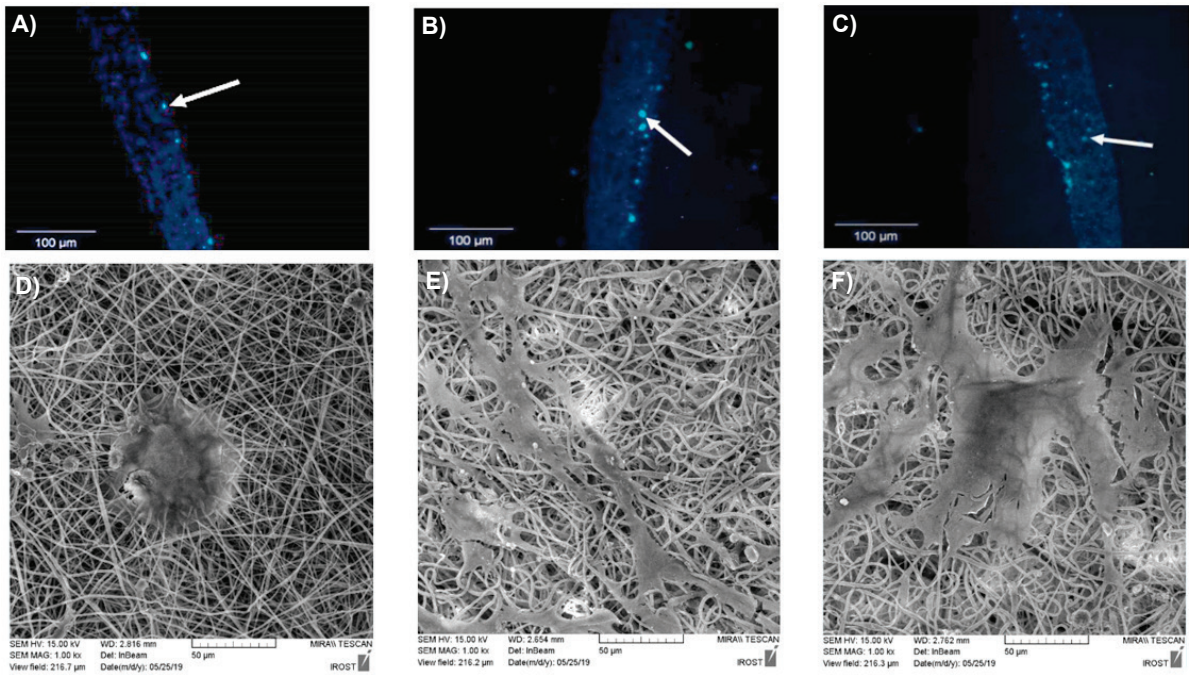

Figure 4. Cell infiltration in electrospun scaffolds, after one week of culture for **A)** control, **B)** PCL-nHA:gelatin 90:10 after the treatment, **C)** PCL-nHA:gelatin 80:20 after the treatment. SEM images of the cellular expansion on the scaffolds, **D)** control, **E)** PCL-nHA:gelatin, 90:10 after the treatment, and **F)** PCL-nHA:gelatin, 80:20 after the treatment.

the modified scaffolds (PCL-nHA:gelatin, 90:10 and 80:20) triggered more expression of COL1, OCN and Runx2 compared to the unmodified scaffolds (**Fig. 3C-3E**). No significant difference was observed between the two modified groups, but both groups represented a significant difference compared to the unmodified scaffolds.

5. Discussion

The use of electrospun scaffolds in bone tissue engineering has been useful owing to its potential to mimic the nano-architecture of bone. However, as a "3D architecture", this kind of scaffold cannot provide suitable conditions for cell infiltration, due to small pore size (32-34). Increase of the pore size of electrospun scaffolds using sacrificial fibers to solve the problem of cell infiltration by PEO was the subject of many previous investigations, but high cost of PEO encouraged them to find cheaper and more affordable sacrificing agents (14, 25, 35, 36). Here, we investigated a combination of gelatin as a sacrificial agent and ultrasonication in PCL-nHA electrospun scaffolds for bone tissue engineering. As expected, by increasing the amount of gelatin, the total pore area became larger, which is approximately similar to PEO. For modified PCL-nHA:PEO (PEO removal and ultrasonication), 90:10 and 80:20, Aghajanpoor *et al*. reached the pore areas of 45.80 and 51.43 μm^2, respectively, which were 2.8- and 3.4-fold higher than those of the unmodified group (PCL-nHA with the pore area of 15.77 μm^2), respectively (14). Phipps *et al*. increased the pore area for TRI (PCL/Col/nHA) scaffolds using PEO. With a weight ratio of 25%, PEO was removed as a sacrificial agent, and the pore area was increased from 422 μm^2 to 1826 μm^2, being approximately a 4-fold increase (35). By comparing the increase in the pore area due to removal of gelatin and PEO in our preliminary experiments (not presented here), it was found that the pore area caused by removal of PEO was higher (for PCL-nHA:gelatin and PCL-nHA:PEO, 80:20, the total pore area was increased

2.8- and 3.4-fold compared to the unmodified scaffold, respectively). It could be related to the incomplete removal of gelatin from the construct and the other structural and physical differences between gelatin and PEO.

Pore distribution is one of the most important points in the case of pore size increase. In fact, by increasing the number of larger pores, possibility of the cell infiltration into the internal parts of the scaffold increases. By increasing the number of pore areas between 10-20 μm^2 from 9% (for PCL-nHA:gelatin, 90:10 after treatment) to 33% (for PCL-nHA:gelatin, 80:20 after treatment), cell infiltration was increased from 35.2±5.7 μm to 42.7±4.6 μm, respectively.

The FTIR results and contact angle analysis indicated partial removal of gelatin in the modified scaffolds. Although the amount of residual gelatin in the scaffold was very small, it is possible to be completely removed by rinsing at a higher ambient temperature. The presence of a low amount of gelatin in the scaffold after modification, regarding no obvious observation of gelatin fibers in the SEM images and its small peak in 1637 cm^{-1}, caused hydrophilicity of the scaffold. The hydrophilicity of PCL-nHA scaffolds without plasma treatment was due to the small amount of gelatin in the structure. Whited *et al*. showed surface mineralization of poly ($_L$-Lactic Acid) (PLLA) scaffolds after PEO removal, by submersion in simulated body fluid (SBF) (36). The residual gelatin, in addition to making hydrophilic scaffolds, is suitable for cell adhesion and biocompatibility of scaffolds in the cell culture process. As expected, the mechanical properties were decreased after modification (gelatin removal and ultrasonication), being similar to PEO removal (14, 25, 37). The relative stress for PCL-nHA:PEO, 80:20 after the treatment in our previous work ,0.62 (14), was similar to that one in the present study. In using gelatin (PCL-nHA:gelatin 80:20 after treatment), the stress was 0.64. Although higher mechanical strength is more suitable, the mechanical properties can be improved during maturation of the cells and scaffolds by the ECM secreted from the infiltrated cells.

Proliferation of the cells on the modified scaffolds compared to TCP and unmodified groups indicated the effect of more space created for cell growth and proliferation. Lower growth of the cells on TCP and the unmodified group from day 14 to 21 was obvious, but an increasing trend was observed for the modified scaffolds. Wang et al. observed that between days 4 and 9, no growth or proliferation was observed for cells cultured on unmodified PCL scaffolds, but this was the case for modified scaffolds, and the cells proliferated in contrast to the unmodified state. In fact, the constructed "3D architecture" is essential for this phenomenon (38).

The results of the ALP activity and expression of collagen type I, runx2 and OCN genes indicated the appropriate osteogenesis properties of the modified scaffolds. On day 14, the ALP activity was increased 2.7-fold compared to the control group. There was no significant difference in the ALP activity between the two modified groups due to an almost similar total pore area. Apparently, larger pore sizes improved the cellular infiltration, and higher cell-cell and cell-scaffold interactions enhanced the expression of collagen type I, runx 2 and OCN 2.3, 2.4 and 3.1 folds, respectively, compared to the control group on day 14.

Similar to ALP activity results, there was no significant difference between the two modified groups. Other researchers indicated the upregulation of osteogenic related genes due to increased pore size (39). Aghajanpoor *et al*. reported 1.86, 2.54 and 2.16 folds increases in the ALP activity and the expression of OCN and collagen type I, respectively compared to the control group on day 14 (for modified PCL-nHA:PEO 80:20) (14). Whited *et al*. reported a double increase in the OCN expression during days 10-14 in modified PLLA scaffolds compared to the control group (36).

By comparing the ALP activity and the expression of bone related genes in the present study to those reported by Aghajanpoor and Whited, it could be concluded that osteogenic behaviors are more appropriate if gelatin is used as a sacrificial agent. This increment may be due to the residual amount of gelatin in the structure, which improves the biomimetic of the scaffolds; however, the increased pore area by removal of PEO was higher than that by gelatin. In fact, the differentiation, pore area and proliferation of the cells are closely associated with each other. Therefore, the results of the MTT assay showed less proliferation, and these issues increased osteogenic behaviors.

The results of morphological analysis, mechanical properties, FTIR, MTT assay, ALP activity, cellular infiltration and real-time RT-PCR demonstrated that gelatin was an inexpensive and more affordable substitute for PEO to enhance the average pore size of electrospun PCL-nHA scaffolds.

6. Conclusions

The present study aimed to use a cheaper and more available polymer as a sacrificial agent to increase the pore size of electrospun PCL-nHA scaffolds. The results indicated that co-electrospinning of gelatin and PCL-nHA was performed well, and the scaffold treatment (gelatin removal and ultrasonication) increased the pore size, causing it to be suitable for bone tissue engineering. FTIR and contact angle measurements revealed incomplete gelatin removal. Furthermore, these small amounts of gelatin enhanced the biomimetic and biocompatibility of the scaffold. Moreover, since the scaffold was hydrophilic, no plasma treatment was required. Scaffold treatment reduced mechanical properties, but the benefits gained from this reduction were more significant. However, the scaffold has remained mechanically suitable for bone tissue engineering. The use of gelatin as a novel sacrificial agent in PCL-nHA nanofibrous scaffolds increased cell infiltration and proliferation and promoted osteogenic properties. Our findings demonstrated the suitability of gelatin as a sacrificial agent to enhance the pore size of electrospun scaffolds in bone tissue engineering.

Funding

This work was supported by Tarbiat Modares University and Royan Institute.

References

1. Wang M, Park S, Nam Y, Nielsen J, Low SA, Srinivasarao M, *et al*. Bone-fracture-targeted dasatinib-oligoaspartic acid conjugate potently accelerates fracture repair. *Bioconjugate Chem*. 2018;**29**(11):3800-3809. doi:10.1021/acs.bioconjchem.8b00660.
2. Iyer KM. Anatomy of Bone, Fracture, and Fracture Healing: *Springer*. 2019. 1-17 p. doi:10.1007/978-3-030-15089-1_1.
3. Baroli B. From natural bone grafts to tissue engineering therapeutics: brainstorming on pharmaceutical formulative requirements and challenges. *J Pharm Sci*. 2009;**98**(4):1317-1375. doi:10.1002/jps.21528.
4. Amini AR, Laurencin CT, Nukavarapu SP. Bone tissue engineering: recent advances and challenges. *Crit Rev Biomed Eng*. 2012;**40**(5). doi:10.1615/CritRevBiomedEng.v40.i5.10.
5. Yu X, Tang X, Gohil SV, Laurencin CT. Biomaterials for bone regenerative engineering. *Adv Healthc Mater*. 2015;**4**(9):1268-1285. doi:10.1002/adhm.201400760.
6. Haugen HJ, Lyngstadaas SP, Rossi F, Perale G. Bone grafts: which is the ideal biomaterial? *J Clin Periodontol*. 2019;**46**:92-102. doi:10.1111/jcpe.13058.
7. Vacanti JP, Langer R. Tissue engineering: the design and fabrication of living replacement devices for surgical reconstruction and transplantation. *The Lancet*. 1999;**354**:S32-S34. doi:10.1016/S0140-6736(99)90247-7.
8. Meinel L, Karageorgiou V, Fajardo R, Snyder B, Shinde-Patil V, Zichner L, *et al*. Bone tissue engineering using human mesenchymal stem cells: effects of scaffold material and medium flow. *Ann Biomed Eng*. 2004;**32**(1):112-122. doi:10.1023/B:ABME.0000007796.48329.b4.
9. Bose S, Roy M, Bandyopadhyay A. Recent advances in bone tissue engineering scaffolds. *Trends Biotechnol*. 2012;**30**(10):546-554. doi:10.1016/j.tibtech.2012.07.005.
10. Cheng A, Schwartz Z, Kahn A, Li X, Shao Z, Sun M, *et al*. Advances in porous scaffold design for bone and cartilage tissue engineering and regeneration. *Tissue Eng Part B Rev*. 2019;**25**(1):14-29. doi:10.1089/ten.teb.2018.0119.
11. Alonzo M, Primo FA, Kumar SA, Mudloff JA, Dominguez E, Fregoso G, *et al*. Bone tissue engineering techniques, advances, and scaffolds for treatment of bone defects. *Current Opinion in Biomedical Engineering*. 2021;**17**:100248. doi:10.1016/j.cobme.2020.100248.
12. Subbiah T, Bhat GS, Tock RW, Parameswaran S, Ramkumar SS. Electrospinning of nanofibers. *J Appl Polym Sci*. 2005;**96**(2):557-569. doi:10.1002/app.21481.
13. Ameer JM, Pr AK, Kasoju N. Strategies to tune electrospun scaffold porosity for effective cell response in tissue engineering. *J Funct Biomater*. 2019;**10**(3):30. doi:10.3390/jfb10030030.
14. Aghajanpoor M, Hashemi-Najafabadi S, Baghaban-Eslaminejad M, Bagheri F, Mohammad Mousavi S, Azam Sayyahpour F. The effect of increasing the pore size of nanofibrous scaffolds on the osteogenic cell culture using a combination of sacrificial agent electrospinning and ultrasonication. *J Biomed Mater Res A*. 2017;**105**(7):1887-1899. doi:10.1002/jbm.a.36052.
15. Rahmani A, Hashemi-Najafabadi S, Eslaminejad MB, Bagheri F, Sayahpour FA. The effect of modified electrospun PCL-nHA-nZnO scaffolds on osteogenesis and angiogenesis. *J Biomed Mater Res A*. 2019;**107**(9):2040-2052. doi:10.1002/jbm.a.36717.
16. Hadida M, Marchat D. Strategy for achieving standardized bone models. *Biotechnol Bioeng*. 2020;**117**(1):251-271. doi:10.1002/bit.27171.
17. Yaghoobi M, Hashemi-Najafabadi S, Soleimani M, Vasheghani-Farahani E. Osteogenic induction of human mesenchymal stem cells in multilayered electrospun scaffolds at different flow rates and configurations in a perfusion bioreactor. *J Biosci Bioeng*. 2019;**128**(4):495-503. doi:10.1016/j.jbiosc.2019.03.015.
18. Yang X, Wang Y, Zhou Y, Chen J, Wan Q. The Application of Polycaprolactone in Three-Dimensional Printing Scaffolds for Bone Tissue Engineering. *Polymers*. 2021;**13**(16):2754. doi:10.3390/polym13162754.
19. Dwivedi R, Kumar S, Pandey R, Mahajan A, Nandana D, Katti DS, *et al*. Polycaprolactone as biomaterial for bone scaffolds: Review of literature. *Journal of Oral Biology and Craniofacial Research*. 2020;**10**(1):381-388. doi:10.1016/j.jobcr.2019.10.003.
20. Ju YM, San Choi J, Atala A, Yoo JJ, Lee SJ. Bilayered scaffold for engineering cellularized blood vessels. *Biomaterials*. 2010;**31**(15):4313-4321. doi:10.1016/j.biomaterials.2010.02.002.
21. Ki CS, Park SY, Kim HJ, Jung H-M, Woo KM, Lee JW, et al. Development of 3-D nanofibrous fibroin scaffold with high porosity by electrospinning: implications for bone regeneration. *Biotechnology Letters*. 2008;**30**(3):405-410. doi:10.1007/s10529-007-9581-5.
22. Rnjak-Kovacina J, Weiss AS. Increasing the pore size of electrospun scaffolds. *Tissue Eng Part B Rev*. 2011;**17**(5):365-

372. doi:10.1089/ten.teb.2011.0235.
23. Lee JB, Jeong SI, Bae MS, Yang DH, Heo DN, Kim CH, *et al*. Highly porous electrospun nanofibers enhanced by ultrasonication for improved cellular infiltration. *Tissue Eng Part A*. 2011;**17**(21-22):2695-2702. doi:10.1089/ten.tea.2010.0709.
24. Jeong SI, Burns NA, Bonino CA, Kwon IK, Khan SA, Alsberg E. Improved cell infiltration of highly porous 3D nanofibrous scaffolds formed by combined fiber–fiber charge repulsions and ultra-sonication. *J Mater Chem B*. 2014;**2**(46):8116-8122. doi:10.1039/C4TB01487A.
25. Baker BM, Gee AO, Metter RB, Nathan AS, Marklein RA, Burdick JA, *et al*. The potential to improve cell infiltration in composite fiber-aligned electrospun scaffolds by the selective removal of sacrificial fibers. *Biomaterials*. 2008;**29**(15):2348-2358. doi:10.1016/j.biomaterials.2008.01.032.
26. Hodge J, Quint C. The improvement of cell infiltration in an electrospun scaffold with multiple synthetic biodegradable polymers using sacrificial PEO microparticles. *J Biomed Mater Res A*. 2019;**107**(9):1954-1964. doi:10.1002/jbm.a.36706.
27. Yang W, Yang F, Wang Y, Both SK, Jansen JA. In vivo bone generation via the endochondral pathway on three-dimensional electrospun fibers. *Acta Biomater*. 2013;**9**(1):4505-4512. doi: 10.1016/j.actbio.2012.10.003.
28. Papadopoulou S, Tsioptsias C, Pavlou A, Kaderides K, Sotiriou S, Panayiotou C. Superhydrophobic surfaces from hydrophobic or hydrophilic polymers via nanophase separation or electrospinning/ electrospraying. *Colloids Surf A: Physicochem Eng Asp*. 2011;**387**(1-3):71-78. doi:10.1016/j.colsurfa.2011.07.028.
29. Gaspar-Pintiliescu A, Stanciuc A-M, Craciunescu O. Natural composite dressings based on collagen, gelatin and plant bioactive compounds for wound healing: A review. *Int J Biol Macromol*. 2019;**138**:854-865. doi:10.1016/j.ijbiomac.2019.07.155.
30. Montgomery AB, McClinton A, Nair L, Laurencin CT. Nail matrix regenerative engineering: in vitro evaluation of poly (lactide-co-glycolide)/gelatin fibrous substrates. *J Biomed Mater Res A*. 2020;**108**(5):1136-1143. doi:10.1002/jbm.a.36888.
31. Udomluck N, Koh W-G, Lim D-J, Park H. Recent developments in nanofiber fabrication and modification for bone tissue engineering. *Int J Mol Sci*. 2020;**21**(1):99. doi:10.3390/ ijms21010099.
32. Li WJ, Danielson KG, Alexander PG, Tuan RS. Biological response of chondrocytes cultured in three-dimensional nanofibrous poly (ϵ-caprolactone) scaffolds. *J Biomed Mater Res A*. 2003;**67**(4):1105-1114. doi:10.1002/jbm.a.10101.
33. Lin W, Chen M, Qu T, Li J, Man Y. Three-dimensional electrospun nanofibrous scaffolds for bone tissue engineering. *J Biomed Mater Res Part B Appl Biomater*. 2020;**108**(4):1311-1321. doi:10.1002/jbm.b.34479.
34. Nair LS, Bhattacharyya S, Laurencin CT. Development of novel tissue engineering scaffolds via electrospinning. *Expert Opin Biol Ther*. 2004;**4**(5):659-668. doi:10.1517/14712598.4.5.659.
35. Phipps MC, Clem WC, Grunda JM, Clines GA, Bellis SL. Increasing the pore sizes of bone-mimetic electrospun scaffolds comprised of polycaprolactone, collagen I and hydroxyapatite to enhance cell infiltration. *Biomaterials*. 2012;**33**(2):524-534. doi:10.1016/j.biomaterials.2011.09.080.
36. Whited BM, Whitney JR, Hofmann MC, Xu Y, Rylander MN. Pre-osteoblast infiltration and differentiation in highly porous apatite-coated PLLA electrospun scaffolds. *Biomaterials*. 2011;**32**(9):2294-2304. doi:10.1016/j.biomaterials.2010.12.003.
37. Wang K, Xu M, Zhu M, Su H, Wang H, Kong D, *et al*. Creation of macropores in electrospun silk fibroin scaffolds using sacrificial PEO-microparticles to enhance cellular infiltration. *J Biomed Mater Res A*. 2013;**101**(12):3474-3481. doi:10.1002/ jbm.a.34656.
38. Wang K, Zhu M, Li T, Zheng W, Xu LL, Zhao Q, *et al*. Improvement of cell infiltration in electrospun polycaprolactone scaffolds for the construction of vascular grafts. *J Biomed Nanotechnol*. 2014;**10**(8):1588-1598. doi:10.1166/jbn.2014.1849.
39. Phadke A, Hwang Y, Kim SH, Kim SH, Yamaguchi T, Masuda K, *et al*. Effect of scaffold microarchitecture on osteogenic differentiation of human mesenchymal stem cells. *Eur Cells Mater*. 2013;**25**:114. doi:10.22203/ecm.v025a08.